



Published in final edited form as:

*Nat Mater.* 2007 May ; 6(5): 385–392. doi:10.1038/nmat1890.

## Multifunctional chondroitin sulphate for cartilage tissue-biomaterial integration

DONG-AN WANG<sup>1,2</sup>, SHYNI VARGHESE<sup>1</sup>, BLANKA SHARMA<sup>1,3</sup>, IOSSIF STREHIN<sup>1</sup>, SARA FERMANIAN<sup>1,3</sup>, JUSTIN GORHAM<sup>4</sup>, D. HOWARD FAIRBROTHER<sup>4</sup>, BRETT CASCIO<sup>5</sup>, JENNIFER H. ELISSEFF<sup>1,5,\*</sup>

<sup>1</sup>Department of Biomedical Engineering, Johns Hopkins University, Baltimore, Maryland 21218, USA

<sup>2</sup>Division of Bioengineering, School of Chemical and Biomedical Engineering, Nanyang Technological University, Singapore 637457

<sup>3</sup>Cartilix, Inc., Foster City, California 94404, USA

<sup>4</sup>Department of Chemistry, Johns Hopkins University, Baltimore, Maryland 21218, USA

<sup>5</sup>Department of Orthopedics, Johns Hopkins Medical School, Baltimore, Maryland 21218, USA

### Abstract

A biologically active, high-strength tissue adhesive is needed for numerous medical applications in tissue engineering and regenerative medicine. Integration of biomaterials or implants with surrounding native tissue is crucial for both immediate functionality and longterm performance of the tissue. Here, we use the biopolymer chondroitin sulphate (CS), one of the major components of cartilage extracellular matrix, to develop a novel bioadhesive that is readily applied and acts quickly. CS was chemically functionalized with methacrylate and aldehyde groups on the polysaccharide backbone to chemically bridge biomaterials and tissue proteins via a twofold covalent link. Three-dimensional hydrogels (with and without cells) bonded to articular cartilage defects. In *in vitro* and *in vivo* functional studies this approach led to mechanical stability of the hydrogel and tissue repair in cartilage defects.

---

Reparative medicine requires the bonding of diverse tissues as we seek to enhance structure and deliver new materials to failing body parts. Currently, surgical integration of tissues is generally carried out using sutures and/or applying a tissue adhesive. There are a number of adhesives that are used clinically including derivatives of cyanoacrylates (Superglue)<sup>1-3</sup>, Bioglue (gluteraldehyde–albumin)<sup>4,5</sup> and fibrin glue (Tisseal)<sup>6-8</sup>. Although these adhesives

---

Reprints and permission information is available online at <http://npg.nature.com/reprintsandpermissions/>

\*Correspondence and requests for materials should be addressed to J.H.E. [jhe@jhu.edu](mailto:jhe@jhu.edu).

Author contributions

D.W. was responsible for synthesis. S.V., I.S., J.G. and D.F. were responsible for chemical analysis. B.S., S.F. and B.C. were responsible for rabbit and goat studies. J.H.E. was responsible for design, data analysis and manuscript preparation.

Supplementary Information accompanies this paper on [www.nature.com/naturematerials](http://www.nature.com/naturematerials).

Competing financial interests

The authors declare competing financial interests: details accompany the full-text HTML version of the paper at [www.nature.com/naturematerials/](http://www.nature.com/naturematerials/).

have some efficacy, they suffer from poor biocompatibility or insufficient bonding strength. Furthermore, there is no bonding technique or adhesive that performs adequately in the challenging area of orthopaedics.

An optimal integration method would tightly bond tissues, be quickly and easily applied clinically, demonstrate biocompatibility and promote tissue repair. Currently, there are limited surgical methods and no adhesive that is capable of bonding or integrating cartilage tissue. Chondroitin sulphate (CS) is a polysaccharide found in cartilage and other tissues in the body. CS has a number of useful biological properties for tissue integration including anti-inflammatory activity<sup>9,10</sup>, water and nutrient absorption<sup>11</sup>, improved wound healing and biological activity at the cellular level that may help to restore arthritic joint function<sup>12,13</sup>. An ideal adhesive would also, at least temporarily, be part of a reconstructive scaffold and share properties of the host tissue. Such a material would require a robust but degradable chemical bond, and the potential to have its bonding tailored to fit specific situations.

Here, integration between biomaterials and tissues was achieved using a novel multifunctional CS. Chondroitin sulphate was chemically functionalized with both methacrylate and aldehyde groups to form two functional arms: one arm to covalently bond to a biomaterial scaffold and the second arm bonding to the tissue surface. This multifunctional CS provides a biologically active and mechanically functional bridge with tissues. To translate this technology to orthopaedic tissue repair, we have applied the CS adhesive to integrate biomaterials with cartilage *in vitro* and *in vivo* to facilitate cartilage repair.

CS was multifunctionalized with methacrylate and aldehyde groups, respectively. First, methacrylate groups were conjugated to CS using glycidyl methacrylate to form methacrylated chondroitin sulphate (CSMA)<sup>14-16</sup>. NMR analysis confirmed that 12% of the CS disaccharides were substituted with methacrylate groups (Fig. 1c). The methacrylate groups polymerize via a radical mechanism and form a crosslinked network. Second, adjacent hydroxyls on the CS polysaccharide backbone (rings) were oxidized with sodium periodate to form aldehyde groups with a substitution efficiency of 70% (percentage of oxidized CS disaccharide repeating units), as confirmed by a hydroxylamine hydrochloride titration<sup>14-16</sup>. The aldehyde functionality of the CS adhesive conjugates with amines present on tissue surfaces via a Schiff-base reaction<sup>17</sup>. The aldehyde and methacrylate groups are both randomly distributed along the polysaccharide chains. The multifunctional CS serves as a 'tissue primer' that forms a covalent bridge between an acrylate-based polymer and a tissue surface. The application of the CS adhesive can be compared to a paint primer that integrates the paint (polymeric grafts) to a wall (host tissues). The complete structure of the adhesive and chemical analysis is described in Fig. 1.

Cartilage repair is a uniquely challenging application where there is a significant need for a tissue integration method. Cartilage is made of a thick matrix of proteoglycans and collagen and this dense lubricating tissue is particularly challenging for adhesives and bonding strategies<sup>18,19</sup>. *In vitro* efficacy of the CS adhesive was evaluated in a model cartilage system where poly(ethylene glycol) diacrylate (PEGDA) hydrogels were bonded to an articular cartilage explant. The only surgical option today, sutures or tacks, creates new

defects in cartilage tissue that will not repair and will remain in the tissue indefinitely<sup>19</sup>. Application of the CS adhesive does not penetrate or damage the cartilage tissue and is simple to administer (Fig. 2a). The CS adhesive is applied to the surface of cartilage using a cotton swab or brush (Fig. 2a, Step 1). A macromer (pregel) solution containing a biocompatible initiator<sup>20</sup> can then be applied to the tissue and polymerized with light (Fig. 2a, Step 2). The hydrogels can be formed with or without suspended cells to generate cellular or acellular implants. An example of a model cartilage–hydrogel construct bonded with the CS adhesive is shown in Fig. 2b. The adhesive can be extended to bonding of other biomaterials containing any vinyl functional group and crosslinked using a number of mechanisms such as redox or chemical initiators, demonstrating the wide applicability and generality of the system.

The integration of the CS adhesive and cartilage tissue was monitored by chemical analysis at the tissue interface using attenuated total reflection Fourier transform infrared (ATR-FTIR, Fig. 1a) spectroscopy<sup>21</sup>. The ATR-FTIR spectrum of untreated cartilage has typical peaks of the protein amide-I at 1,640  $\text{cm}^{-1}$ , amide-II at 1,550  $\text{cm}^{-1}$  and amide-III at 1,240  $\text{cm}^{-1}$  (spectrum 1). The individual matrix component, CS, is distinguished by saccharide alkyls at 2,920 and 1,415  $\text{cm}^{-1}$ , and alkoxylys at 1,030  $\text{cm}^{-1}$  (spectrum 2). When the CS is modified with the functional groups, a new infrared band associated with the C=O stretch appears at 1,730  $\text{cm}^{-1}$  (spectrum 3). Finally, when the CSMA aldehyde is reacted with the cartilage surface and thoroughly washed, the spectrum demonstrated both characteristics of cartilage and the CS adhesive, confirming the presence of the adhesive on the surface of the cartilage (spectrum 4).

The chemical composition of native cartilage and cartilage treated with CS adhesive was further characterized by X-ray photoelectron spectroscopy<sup>22</sup> (XPS). The C(1s) XPS regions of native cartilage and cartilage treated with the CS adhesive are shown in Fig. 1c. The cartilage treated with CS adhesive exhibited a higher concentration of C=O and C—O species, consistent with the fact that the proteoglycan-rich CS-adhesive layer contains significantly more oxygen molecules in both the sugar ring and pendant alcohol groups compared with the native cartilage tissue (Fig. 1c). To estimate the thickness of the CS-adhesive layer, Ar<sup>+</sup> sputtering/etching was carried out in conjunction with XPS. Results from this analysis are shown in Fig. 1d. For Ar<sup>+</sup> sputter times less than 60 min, the atomic percentage of carbon at the surface decreases, whereas the atomic oxygen percentage exhibits a concomitant increase. For sputter times in excess of 60 min, the atomic percentage of oxygen and carbon at the surface remained constant at values similar to those measured for the untreated cartilage surface. This supports the idea that after 60 min of Ar<sup>+</sup> sputtering, the adhesive layer had been removed from the surface of the cartilage (Fig. 1d). To calibrate the rate of CS-adhesive removal by Ar<sup>+</sup> ions, separate sputtering experiments were carried out on a thin film of adhesive deposited on a sputtercleaned gold substrate (see Supplementary Information and the Methods section). Results from these experiments indicate that the CS-adhesive layer thickness is less than 100nm before addition of the hydrogel scaffold.

Cytocompatibility of the adhesive was evaluated by testing the viability of cells in contact with the CS adhesive in the cartilage and in a hydrogel bonded to the tissue surface. Live–

dead (calcein–ethidium dye) cell staining indicated that the cells encapsulated in the hydrogel and the chondrocytes residing in the cartilage explant adjacent to the adhesive remained viable (stained fluorescent green with calcein) over 5 weeks of culture (Fig. 2c). Further *in vivo* compatibility of the constructs was assessed by implantation in a small-animal model and subsequent *in situ* application in the joint space of a mid-size- and large-animal model.

Hydrogels have been used as vehicles for delivery and maintenance of cells or bioactive factors for cartilage repair. Chondrocytes, mesenchymal stem cells and embryonic stem cells encapsulated in hydrogels form cartilage-like tissue *in vitro* and *in vivo* after subcutaneous implantation<sup>23–25</sup>. Unfortunately, cartilage does not integrate well with transplanted tissues of any kind; either allo-, auto-graft tissue or engineered cartilage. This phenomenon is thought to be due, in part, to the thick extracellular matrix and avascular nature of the tissue<sup>19,26–29</sup>. The challenge for cartilage integration in tissue engineering is twofold: the initial biomaterial scaffold must be stabilized in the joint and the subsequent developing tissue must integrate with the surrounding native tissue. In this *in vitro* study, CS adhesive bound a cell-laden hydrogel to the cartilage surface to promote integration and stability of the implant and developing tissue. Furthermore, as CS also has biological activity, it was hypothesized that incorporation of the CS adhesive would improve cell activity and tissue formation at the hydrogel–cartilage interface. The hydrogel–CS–cartilage model system (Fig. 2b) was applied to carefully evaluate engineered and host cartilage integration *in vitro* and *in vivo* before moving to preclinical studies.

CS-adhesive integration of engineered and native tissue was first characterized *in vitro* by bonding a hydrogel containing primary chondrocytes to a cartilage explant as shown in Figs 2 and 3. After 5 weeks of *in vitro* incubation, new cartilage tissue developed in the hydrogel that was integrated to the cartilage surface (Fig. 3). An extracellular matrix rich in cartilage-specific collagen and proteoglycans was secreted in the hydrogel as visualized by Masson's Trichrome (collagen) and Safranin-O (proteoglycan) staining (Fig. 3b,d). Extracellular matrix secretion at the hydrogel scaffold–cartilage interface was particularly extensive, with new tissue forming that was bonding the cellular hydrogel containing developing tissue with the cartilage explant. Hydrogels without cells remained adhered to the cartilage tissue and contained no extracellular matrix (Fig. 3a,c). Previous studies attempting integration of cartilage found a fibrous cartilage containing Type-I collagen at the tissue interface<sup>27</sup>. Fibrous cartilage is mechanically weaker than hyaline cartilage and is probably the source of failure in cartilage integration. On the contrary, cells at the CS-adhesive–tissue interface stained positive for Type-II collagen and demonstrated some cell-associated matrix production (Fig. 3e). Without CS adhesive, the hydrogel did not adhere to the cartilage and quickly separated from the tissue in culture.

As a preliminary step to evaluate CS-adhesive compatibility and efficacy *in vivo*, integrated hydrogel–CS–cartilage constructs were implanted in the subcutaneous space of athymic mice (Fig. 3f). The CS adhesive successfully bonded the hydrogels (with or without cells) to cartilage tissue explants over a 5 week implantation period (Fig. 3h,i). *In vivo* tissue development and integration correlated with the *in vitro* studies, although tissue production in the hydrogels was slightly decreased owing to limited diffusion and nutrition in the

subcutaneous space. Proteoglycan secretion was again observed in the hydrogel and at the interface (Fig. 3i). Mechanical properties of the developing tissue in the hydrogel and integrated hydrogel–CS–cartilage constructs incubated *in vitro* and *in vivo* increased over time, suggesting the accumulation of functional cartilage tissue (see Supplementary Information, Fig. S1).

The mechanical function of the CS adhesive is critical to its application for tissue integration and adhesion. The hydrogels we apply to tissue repair are designed to support cell viability, nutrientwaste flow and promote fast tissue development. To achieve these characteristics, the hydrogels have a high porosity or lower crosslinking density and therefore limited physical strength<sup>23,24</sup>. Initial evaluation of the CS-adhesive strength demonstrated that the bulk hydrogel failed before the CS-adhesive interface (Fig. 4b). Constructs bonded with the adhesive and exposed to tensile and shear forces did not fail at the interface (Fig. 4b, +CS). Without the adhesive, failure quickly occurred at the hydrogel–cartilage interface (Fig. 4b, –CS). Therefore, to determine the ultimate failure strength of the CS adhesive, a higher strength, highly crosslinked hydroxylethyl methacrylate (HEMA) gel was integrated to cartilage with the adhesive. Tensile and shear forces of 45 and 46 kPa were required to dislocate the HEMA gels from the tissue (Table 1). As this integrative strength already exceeds the bulk strength of the PEGDA hydrogels (40 kPa), the strength of the CS adhesive is more than sufficient for the fixation of hydrogels to the cartilage surface.

The mechanically harsh environment of the joint is another challenge for integrating cartilage tissue with biomaterials or tissue implants. Integration of biomaterials or engineered tissue with native cartilage tissue in the joint will improve implant stability with surrounding host tissue and protect the nascent tissue developing in the joint. Therefore, we first investigated the efficacy and requirement of the CS adhesive in a rabbit model before translating to a larger-animal model for cartilage repair.

Rabbits are a well-accepted mid-size-animal model for evaluating materials in a joint environment<sup>30-32</sup>. Larger-animal models provide a better model of cartilage repair, so we used the rabbit model to determine if the CS adhesive was required to retain a hydrogel in the joint space. PEG-based hydrogels were implanted in chondral defects (3.2mmdiameter) in the femoropatellar groove of New Zealand white rabbits, with or without application of the adhesive.

Advances in magnetic resonance imaging (MRI) and its application in orthopaedics have significantly enhanced our ability to evaluate materials and cartilage repair in the joint. The  $T_2$  (spin–spin relaxation) is a biological parameter determined by unique characteristics of a material or tissue that can be evaluated *in situ*. MRI- $T_2$  assessment carried out on the rabbit joints after 5 weeks revealed that defect spaces were filled with hydrogel and/or new tissue growth when the adhesive was applied (Fig. 4a, +CS), but were empty when the hydrogel was not integrated with the CS adhesive (Fig. 4a, –CS). Quantitative MRI- $T_2$  values were also determined for comparison with the imaging results. According to the  $T_2$  distribution curves, the  $T_2$  level detected from the experimental defects with CS adhesive was approximately 80 ms (Fig. 4a, +CS); in comparison with the  $T_2$  value detected in empty control defects, which ranged between 110 and 120 ms.  $T_2$  values obtained from the defects

implanted with hydrogel without adhesive had similar curves to the empty defects (Fig. 4a, –CS). The higher  $T_2$  values in the empty and hydrogel-filled defects reflect the presence of water/body fluids in the defect. The hydrogel biomaterial has a  $T_2$  value between that of cartilage and water/body fluid. Histological analysis also confirmed enhanced tissue development in the defects treated with adhesive and hydrogel (Fig. 4c), compared with untreated controls (Fig. 4e) and defects treated with hydrogel alone, without adhesive (Fig. 4d).

Implantation of hydrogels in the joint space of rabbits confirmed the requirement of the CS adhesive to hold the material in place and suggested potential improvement in tissue repair. Preclinical testing of cartilage technologies requires the use of larger-animal models to better mimic human repair. To this end, we created critical-size chondral defects (6mm diameter) in goat femoral condyles to mimic the most common cartilage defects found in humans. Because of the challenge in translating cell therapies to clinical use, we applied only the biomaterial scaffold in the cartilage defects in conjunction with marrow stimulation to provide an autologous cell source<sup>33,34</sup>. CS adhesive was applied to the cartilage defects as described in Fig. 2a. After subsequent marrow stimulation, the PEGDA hydrogel was photopolymerized in the defect and bonded to the CS adhesive and tissue surface. Animals were killed after 6 months to evaluate new cartilage growth. Cartilage in the defects treated with adhesive and hydrogel showed significantly greater repair compared with empty, untreated defects after 6 months. Both overall tissue fill and per cent of tissue staining for glycosaminoglycans, determined by histomorphometry, significantly increased in the presence of adhesive and hydrogel. Experimental defects with adhesive and hydrogel produced tissue that grossly filled the majority of the defect (Fig. 5b). Underlying bone was grossly visible in control defects, without adhesive or hydrogel (Fig. 5a). Histologically, the contour of the joint surface was more established in experimental defects and more Safranin-O staining was quantitatively observed. The O'Driscoll histological score also increased in the experimental defects, suggesting improvement in cartilage repair with the adhesive and hydrogel (Fig. 5).

Addressing the challenges of adhesion and integration to cartilage will enhance translation of materials and technologies that promote biological repair. Furthermore, the development of tissue adhesives that not only carry out a desired physical function, but also enhance or guide tissue development and repair, will have a significant impact on a number of surgical interventions.

## EXPERIMENTAL PROTOCOL

### SYNTHESIS OF CS ADHESIVE

CSMA was synthesized as previously described<sup>15,16</sup>. Resulting CSMA (300 mg) was oxidized with sodium periodate (308 mg, Aldrich, Milwaukee, WI) in 5ml of deionized water for 16 h in the dark with vigorous stirring. The product, chondroitin sulphate methacrylate aldehyde (CS adhesive), was purified by filtration with Sephadex G-25 (Sigma) size-exclusion chromatography. The chemical structure of the CS adhesive was verified by proton nuclear magnetic resonance (<sup>1</sup>H NMR, 500 MHz, Varian Associates). The

aldehyde substitution degree was determined using the hydroxylamine hydrochloride titration assay<sup>35</sup>.

## CARTILAGE–HYDROGEL INTEGRATION

The CS-adhesive solution (25% w/v, in deionized water) was placed onto cartilage explants (middle layer of the cartilage collected from fetal bovine femoropatellar groove) for 5 min. Unreacted CS adhesive was rinsed with phosphate buffer saline (PBS, pH 7.4). PEGDA (15% w/v, Mw 3,400 Da, Nektar) macromer solution (in PBS, pH 7.4) was mixed together with 0.05% (w/v) biocompatible photoinitiator Igracure 2959 (Ciba-Geigy). The biocompatibility of the photoinitiator and free-radical polymerization was previously confirmed<sup>20</sup>.

## CHARACTERIZATION OF THE CS LAYER USING X-RAY PHOTOELECTRON SPECTROSCOPY

**Sample preparation.**—To avoid contamination from inherent proteoglycans in the cartilage during XPS analysis, the explants samples were digested using chondroitinase ABC. After washing the digested samples with water, 25% (w/v) CS-adhesive solution was applied to the cartilage for 5 min. Unreacted CS adhesive was washed using distilled water and the explant was lyophilized for 24 h.

**Film characterization using X-ray photoelectron spectroscopy in conjunction with sputter depth profiling.**—XPS analysis was carried out in an ultrahigh vacuum chamber ( $P_{\text{base}} \approx 5 \times 10^{-8}$  torr) using a PHI 5400 XPS system. XPS spectra were acquired using a Mg K $\alpha$  (1,253.6 eV) at a take-off angle of 45°. Depth-profiling experiments were carried out and the sputter rate was calibrated and subsequent adhesive layer thickness was determined (see the Supplementary Information).

**In vitro culture of integrated cartilage and hydrogels.**—Hydrogels were prepared with or without primary chondrocytes (35 million cells ml<sup>-1</sup>) isolated from the same animal as the cartilage explants. The polymer solution was placed on a cartilage explant and exposed to light (365 nm, 5mWcm<sup>-2</sup>) for 5 min to crosslink the polymer and form hydrogels. The resulting hydrogel–CS–cartilage constructs were cultured for 5 weeks as described previously<sup>36</sup>.

**Subcutaneous implantation.**—After *ex vivo* formation, integrated hydrogel–CS–cartilage constructs were implanted subcutaneously in four lateral subcutaneous pockets of athymic mice (National Cancer Institute, Frederick, MD). Constructs were collected after 5 weeks for histology and immunohistochemistry (see Supplementary Information and the Methods section).

**Rabbit implantation.**—The CS adhesive was used to integrate hydrogels to the articular cartilage of New Zealand white rabbits. Two bilateral chondral defects were created on the femoropatellar groove of rabbit hind limbs (3–6 months old, male,  $n = 7$ ). Defects were 3.2mm in diameter and the depth was variable depending on the cartilage thickness and surgical technique. The defects were first treated with 25% (w/v) CS-adhesive solution for 5

min and rinsed with PBS. PEGDA solution was added to the prepared defect and photopolymerized by exposure to light as described above. Control defects included empty defects ( $n=7$ ) and defects filled with hydrogel without CS-adhesive pretreatment ( $n=7$ ). Samples were collected after 5 weeks and processed for histology.

**MRI- $T_2$  mapping and scanning.**—Transverse relaxation time ( $T_2$ ) mapping and scanning were carried out with a medical MRI technique (NMR spectrometer: Bruker DMX 400, proton birdcage resonator: Bruker Analytik GmbH).  $T_2$  maps were generated as described in Supplementary Information and the Methods section. Images were obtained 5 weeks after gel implantation.

**Cartilage repair in goat model.**—Surgery and analysis were carried out using good laboratory practices and with IUACAC approval (Thomas D. Morris, Reisterstown, MD). Two 6 mm chondral defects were created on the central ridge of the medial femoral condyle of the right stifle in caprine (goats, 2–3 years old). Experimental defects ( $n = 12$ , 6 goats) were treated with the CS adhesive. Four holes were drilled into the subchondral bone to provide marrow cell access to the defect site. PEGDA was polymerized in the defect space via a 4 min exposure to light ( $\lambda = 320\text{--}500$  nm,  $I = 4\text{--}5$  mWcm<sup>-2</sup>). The control defects were left empty ( $n = 6$ , 3 goats). The operative limb was immobilized for 2 weeks with a Schroeder Thomas Splint. After 6 months, animals were killed and defects were processed according to standard histological analysis and Safranin-O staining. Sections were analysed by histomorphometry to calculate tissue fill and glycosaminoglycan staining in addition to O'Driscoll scoring by a blinded observer.

**Statistics.**—Statistical analysis was carried out using an unpaired Student's t-test with a confidence level of 0.05. All values are reported as the mean and standard deviation.

## Supplementary Material

Refer to Web version on PubMed Central for supplementary material.

## Acknowledgements

We acknowledge S. Ramaswamy and R. Spencer for MRI access; J. Cooper and S.-h. Moon for use of mechanical analysis facilities; and N. Marcus for assistance in the animal studies and critical review of the manuscript. The authors would like to acknowledge the Materials Science Department at Johns Hopkins University for use of the surface analysis laboratory. This research was financially supported by NIH Grant No. R21 EB002369-01, R01 EB05517-01, the State of Maryland University Technology Development Fund and Cartilix.

## References

1. Leahey AB, Gottsch JD & Stark WJ Clinical experience with N-butyl cyanoacrylate (Nexacryl) tissue adhesive. *Ophthalmology* 100, 173–180 (1993). [PubMed: 8437823]
2. Singer AJ et al. Prospective, randomized, controlled trial of tissue adhesive (2-octylcyanoacrylate) versus standard wound closure techniques for laceration repair. Stony brook octylcyanoacrylate study group. *Acad. Emerg. Med* 5, 94–99 (1998). [PubMed: 9492126]
3. Woodward SC et al. Histotoxicity of cyanoacrylate tissue adhesive in the rat. *Ann. Surg* 162, 113–122 (1965). [PubMed: 14308782]



4. Herget GW et al. Experimental use of an albumin-glutaraldehyde tissue adhesive for sealing pulmonary parenchyma and bronchial anastomoses. *Eur. J. Cardiothorac. Surg* 19, 4–9 (2001). [PubMed: 11163552]
5. Menon NG, Downing S, Goldberg NH & Silverman RP Seroma prevention using an albumin-glutaraldehyde-based tissue adhesive in the rat mastectomy model. *Ann. Plast. Surg* 50, 639–643 (2003). [PubMed: 12783020]
6. Kjaergard HK, Weis-Fogh US, Sorensen H, Thiis J & Rygg I Autologous fibrin glue-preparation and clinical use in thoracic surgery. *Eur. J. Cardiothorac. Surg* 6, 52–54 (1992) discussion 54. [PubMed: 1543604]
7. Owen RJ et al. Percutaneous ablation of an internal iliac aneurysm using tissue adhesive. *Cardiovasc. Intervent. Radiol* 23, 389–391 (2000). [PubMed: 11060370]
8. Dunn CJ & Goa KL Fibrin sealant: A review of its use in surgery and endoscopy. *Drugs* 58, 863–886 (1999). [PubMed: 10595866]
9. Ronca F, Palmieri L, Panicucci P & Ronca G Anti-inflammatory activity of chondroitin sulfate. *Osteoarthritis Cartilage* 6 (suppl. A), 14–21 (1998). [PubMed: 9743814]
10. Pipitone VR Chondroprotection with chondroitin sulfate. *Drugs Exp. Clin. Res* 17, 3–7 (1991). [PubMed: 1914834]
11. Moss M, Kruger GO & Reynolds DC The effect of chondroitin sulfate on bone healing. *Oral Surg. OralMed. OralPathol* 20, 795–801 (1965).
12. Kerzberg EM, Roldan EJ, Castelli G & Huberman ED Combination of glycosaminoglycans and acetylsalicylic acid knee osteoarthritis. *Scand. J. Rheumatol* 16, 377–380 (1987). [PubMed: 3120308]
13. Rovetta G Galactosaminoglycuroglycan sulfate (matrix) in therapy of tibiofibular osteoarthritis of theknee. *Drugs Exp. Clin. Res* 17, 53–57 (1991). [PubMed: 1914837]
14. Bryant SJ, Arthur JA & Anseth KS Incorporation of tissue-specific molecules alters chondrocyte metabolism and gene expression in photocrosslinked hydrogels. *Acta Biomater.* 1, 243–252 (2005). [PubMed: 16701801]
15. Li Q et al. Photocrosslinkable polysaccharides based on chondroitin sulfate. *J. Biomed. Mater. Res. A* 68, 28–33 (2004). [PubMed: 14661246]
16. Li Q et al. Biodegradable and photocrosslinkable polyphosphoester hydrogel. *Biomaterials* 27, 1027–1034 (2006). [PubMed: 16125222]
17. Reyes JM et al. A modified chondroitin sulfate aldehyde adhesive for sealing corneal incisions. *Invest. Ophthalmol. Vis. Sci* 46, 1247–1250 (2005). [PubMed: 15790885]
18. Buckwalter J & Mankin H Articular cartilage part II: Degeneration and osteoarthritis, repair, regeneration, and transplantation. *J. Bone Joint Surg. A* 79, 612–632 (1997).
19. Hunziker EB Articular cartilage repair: Basic science and clinical progress. A review of the current status and prospects. *Osteoarthritis Cartilage* 10, 432–463 (2002). [PubMed: 12056848]
20. Williams CG, Malik AN, Kim TK, Manson PN & Elisseeff JH Variable cytocompatibility of six cell lines with photoinitiators used for polymerizing hydrogels and cell encapsulation. *Biomaterials* 26, 1211–1218 (2005). [PubMed: 15475050]
21. Werner C & Jacobasch HJ Surface characterization of polymers for medical devices. *Int. J. Artif. Organs* 22, 160–176 (1999). [PubMed: 10357245]
22. Mohai M & Bertoti L Calculation of overlayer thickness on curved surfaces based on XPS intensities. *Surf. Interface Anal* 36, 805 (2004).
23. Elisseeff J et al. Photoencapsulation of chondrocytes in poly(ethylene oxide)-based semi-interpenetrating networks. *J. Biomed. Mater. Res* 51, 164–171 (2000). [PubMed: 10825215]
24. Williams CG et al. In vitro chondrogenesis of bone marrow-derived mesenchymal stem cells in a photopolymerizing hydrogel. *Tissue Eng.* 9, 679–688 (2003). [PubMed: 13678446]
25. Hwang NS, Varghese S, Zhang Z & Elisseeff J Chondrogenic differentiation of human embryonic stem cell-derived cells in arginine-glycine-aspartate-modified hydrogels. *Tissue Eng.* 12, 2695–2706 (2006). [PubMed: 16995803]
26. Obradovic B et al. Integration of engineered cartilage. *J. Orthop. Res* 19, 1089–1097 (2001). [PubMed: 11781010]

27. Zhang Z, McCaffery JM, Spencer RG & Francomano CA Growth and integration of neocartilage with native cartilage in vitro. *J. Orthop. Res* 23, 433–439 (2005). [PubMed: 15734259]
28. Ahsan T & Sah RL Biomechanics of integrative cartilage repair. *Osteoarthritis Cartilage* 7, 29–40 (1999). [PubMed: 10367013]
29. DiMicco MA & Sah RL Integrative cartilage repair: Adhesive strength is correlated with collagen deposition. *J. Orthop. Res* 19, 1105–1112 (2001). [PubMed: 11781012]
30. Solchaga LA et al. Treatment of osteochondral defects with autologous bone marrow in a hyaluronan-based delivery vehicle. *Tissue Eng.* 8, 333–347 (2002). [PubMed: 12031121]
31. Freed LE et al. Joint resurfacing using allograft chondrocytes and synthetic biodegradable polymer scaffolds. *J. Biomed. Mater. Res* 28, 891–899 (1994). [PubMed: 7983087]
32. Buckwalter JA & Mankin HJ Articular cartilage repair and transplantation. *Arthritis Rheum.* 41, 1331–1342 (1998). [PubMed: 9704631]
33. Kramer J et al. In vivo matrix-guided human mesenchymal stem cells. *Cell. Mol. Life Sci* 63, 616–626 (2006). [PubMed: 16482398]
34. Mithoefer K et al. Chondral resurfacing of articular cartilage defects in the knee with the microfracture technique. *Surgical technique. J. Bone Joint Surg. Am* 88 (suppl. 1), 294–304 (2006). [PubMed: 16951101]
35. Zhao H & Heindel ND Determination of degree of substitution of formyl groups in polyaldehyde dextran by the hydroxylamine hydrochloride method. *Pharm. Res* 8, 400–402 (1991). [PubMed: 1711201]
36. Guo JF, Jourdan GW & MacCallum DK Culture and growth characteristics of chondrocytes encapsulated in alginate beads. *Connect Tissue Res.* 19, 277–297 (1989). [PubMed: 2805684]

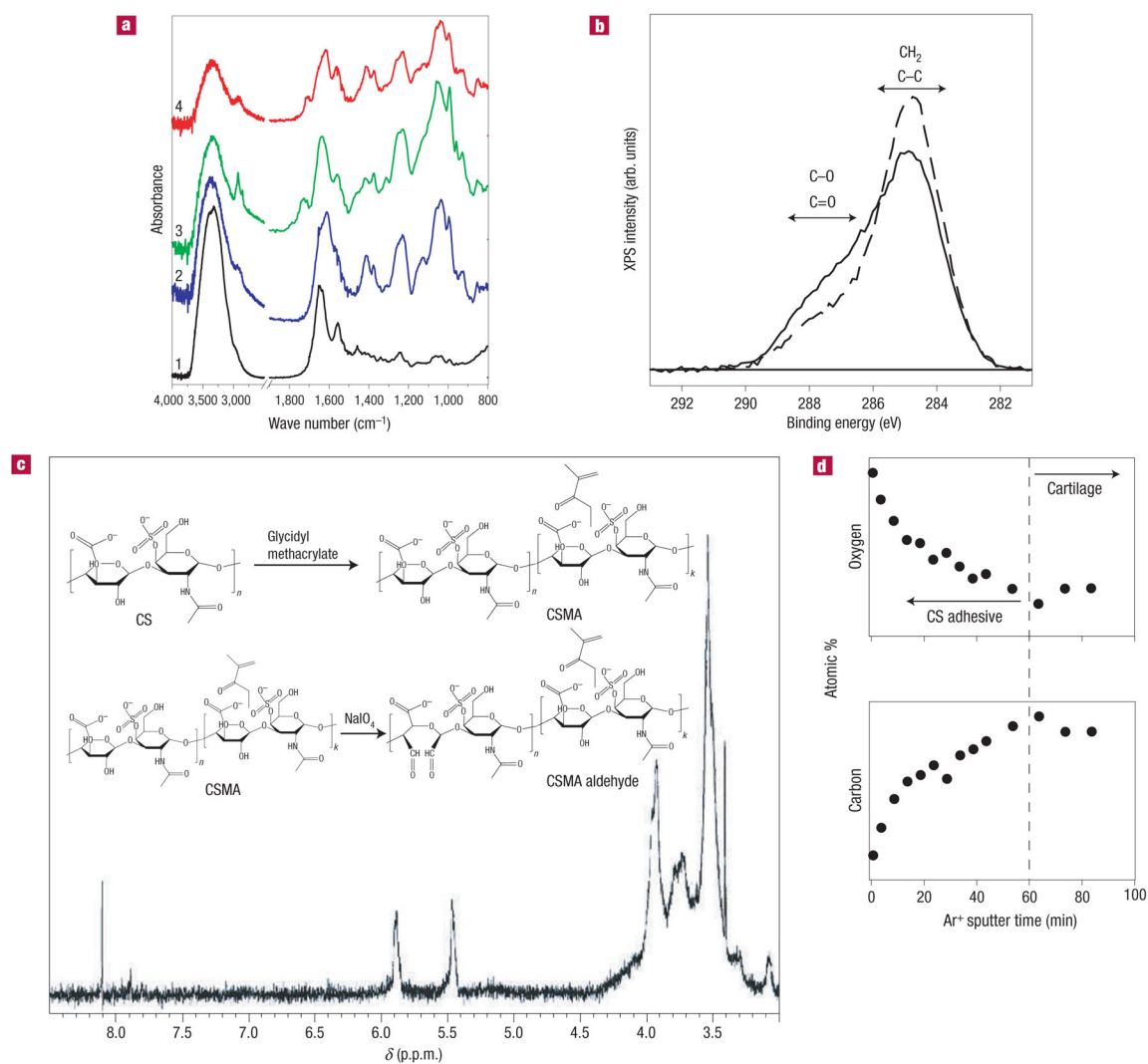


**Figure 1. Synthesis and characterization of CS adhesive.**

**a.** ATR-FTIR spectra indicate the surface of unmodified native cartilage distinguished by stretching bands of protein amide-I at  $1,640\text{ cm}^{-1}$ , amide-II at  $1,550\text{ cm}^{-1}$  and amide-III at  $1,240\text{ cm}^{-1}$  (spectrum 1); unmodified CS with stretching bands of saccharide alkyls at  $2,920$ ,  $2,850$  and  $1,415\text{ cm}^{-1}$  and alkoxylys at  $1,030\text{ cm}^{-1}$  (spectrum 2); CS adhesive with stretching bands of carbonyl at  $1,730\text{ cm}^{-1}$  (spectrum 3); and CS adhesive on the cartilage surface, which contains peaks from both cartilage and the functionalized CS (spectrum 4). **b.** The C(1s) XPS regions of untreated cartilage (dashed line) and cartilage treated with CS adhesive (solid line) exhibit different concentrations of oxygen containing carbon functional groups at the surface. This supports the idea that the CS adhesive is present on the tissue surface. **c.**  $^1\text{H}$  NMR analysis: alkyl protons on saccharide backbone at a chemical shift  $\delta 3.2 \sim 4.0\text{ p.p.m.}$ ; vinyl protons on methacrylate at  $\delta 5.89$  and  $5.44\text{ p.p.m.}$ ; aldehyde protons at  $\delta 8.11\text{ p.p.m.}$  Inset: CS-adhesive synthesis pathway. **d.** Depth profile for a cartilage surface treated with CS adhesive. The tissue was sputtered with  $\text{Ar}^+$  and the variation in the carbon and oxygen content at the surface was measured using XPS. The oxygen and carbon concentration changed over the initial 60 min of sputter time, after which the chemical

composition of the surface remained constant, indicating that all of the adhesive had been removed from the cartilage surface.

Author Manuscript

Author Manuscript

Author Manuscript

Author Manuscript

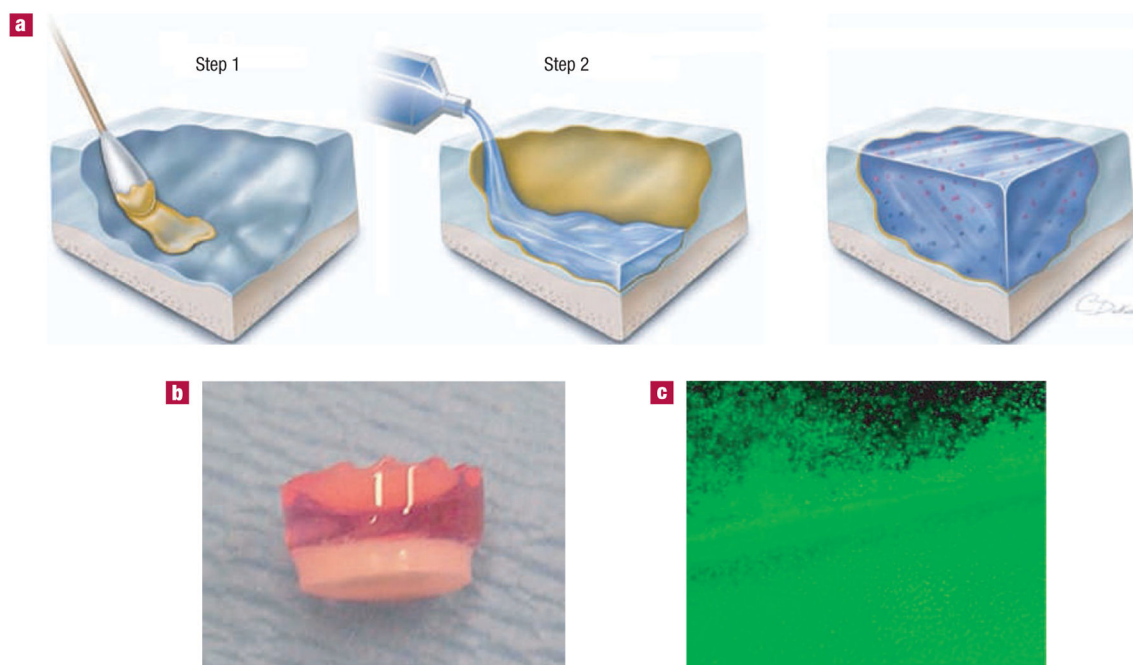


**Figure 2. Schematic diagram of CS-adhesive application and hydrogel integration.**

**a**, The CS adhesive is applied to the cartilage surface with a swab (Step 1). A macromer (pregel) solution is added to the tissue surface modified with the CS adhesive and photopolymerized (Step 2). The resulting hydrogel biomaterial is covalently bound to the cartilage surface via the CS-adhesive bridge. Cells surgically stimulated from the marrow (blue) or exogenously added to the liquid pregel (red) can be incorporated into the hydrogel layer. **b**, Gross picture of a hydrogel bound to cartilage with the CS adhesive. The cartilage tissue is the white, opalescent layer adjacent to the transparent hydrogel layer. Chondrocytes were encapsulated in the hydrogel layer to test the cytocompatibility of the modified CS. **c**, Cells in the hydrogel, adjacent to the CS adhesive, and within the cartilage were viable after 5 weeks of culture, as determined by live–dead fluorescent staining where calcein dye (green) stains only viable cells.

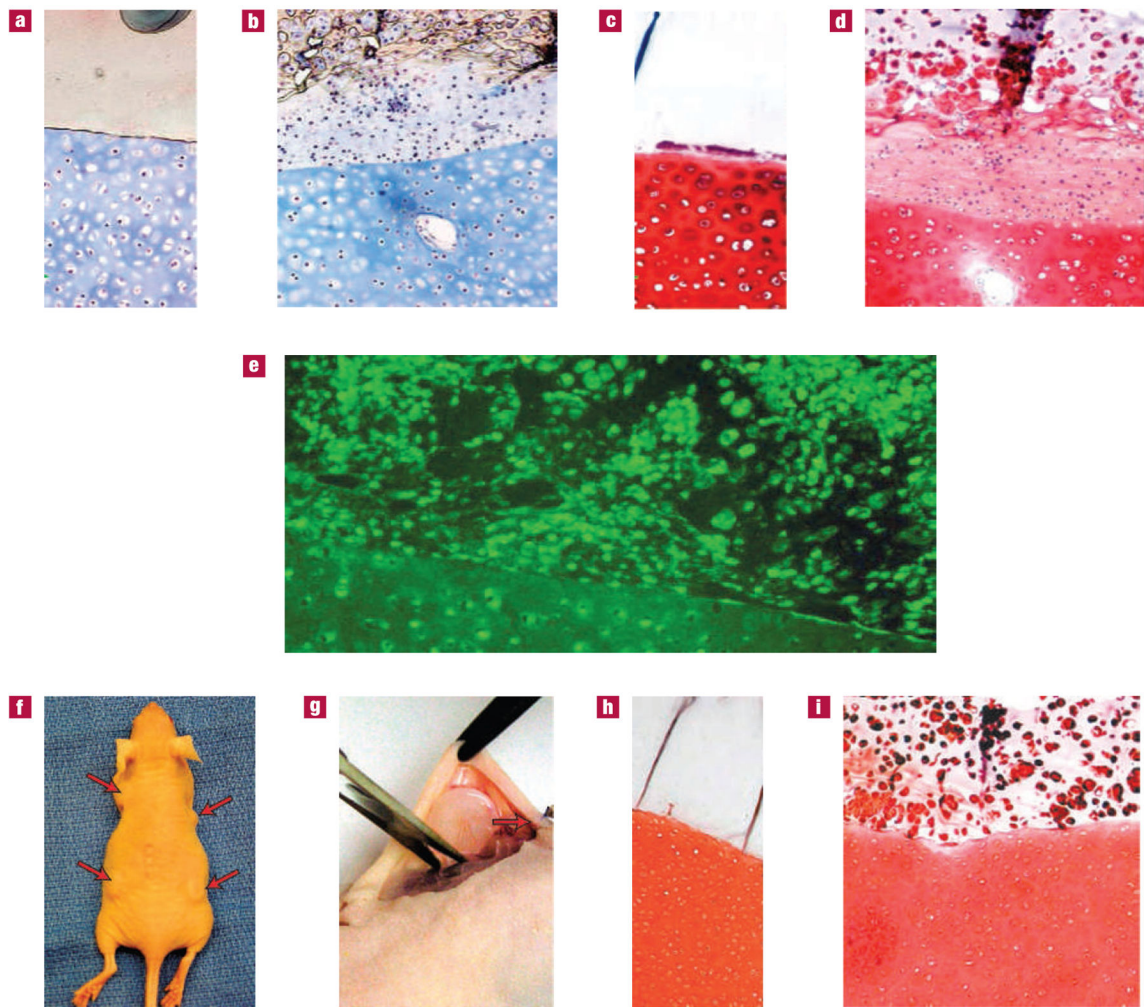


**Figure 3. Integration of hydrogels and developing tissue to the cartilage surface with CS adhesive.**

**a–i,** Hydrogel constructs were bonded to cartilage with the CS adhesive and incubated *in vitro* (**a–e**) or *in vivo* (**f–i**) for 5 weeks. Hydrogels without cells were integrated to cartilage explants and the resulting constructs were stained with Masson's Trichrome (**a**) and Safranin-O (**c**) after *in vitro* culture to visualize collagen and proteoglycans, respectively. The hydrogels remained firmly attached to the cartilage tissue, which also retained cell viability and extracellular matrix. Hydrogels with encapsulated chondrocytes demonstrated total collagen (**b**) and proteoglycan (**d**) production typical of neocartilage. The neocartilage was firmly attached to the cartilage explant. Type-II collagen (**e**), specific to hyaline cartilage, was present in and around cells at the interface and within the native cartilage. Integrated cartilage–hydrogel constructs were also implanted subcutaneously in athymic mice (**f**) and collected after 5 weeks (**g**). Acellular hydrogels remained firmly attached to the cartilage surface without invasion of cells or extracellular matrix production (**h**). Similar to the case for *in vitro* incubation, the hydrogels containing cells produced neocartilage that was bound to the cartilage surface. Proteoglycans (**i**, Safranin-O) were present throughout the hydrogel layer and at the interface of the engineered and native cartilage tissue.

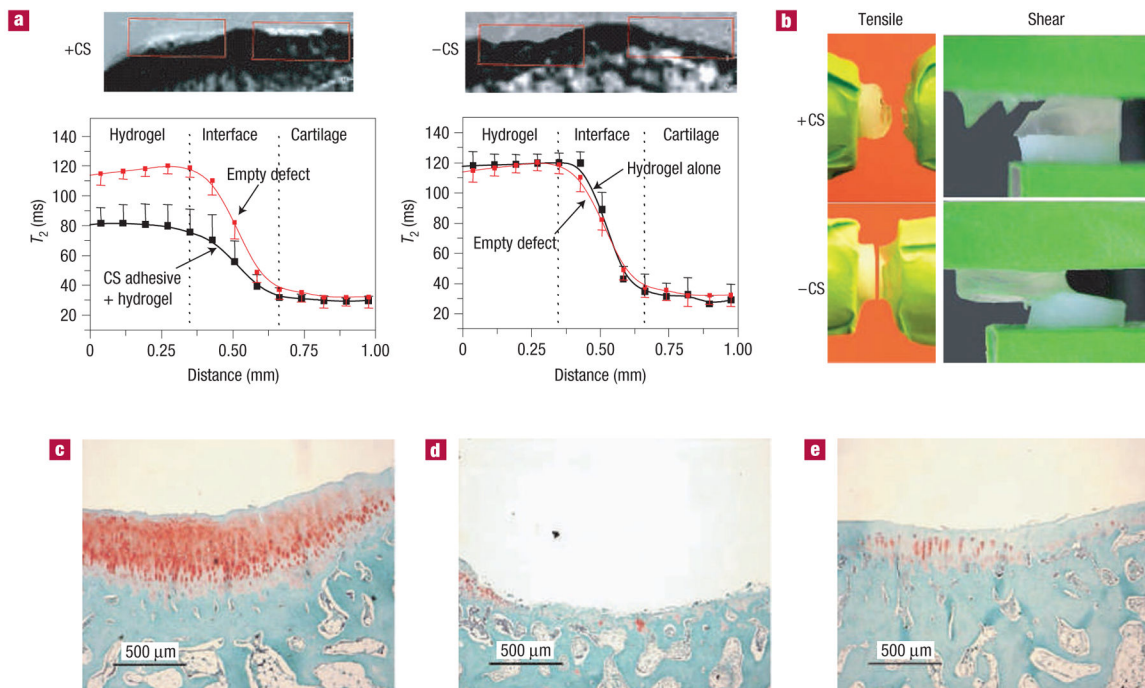


**Figure 4. CS-adhesive mechanical properties and *in vivo* durability.**

Hydrogel was implanted in chondral defects of a rabbit with or without the CS adhesive ( $n = 7$ ). **a**, MRI of the articular defects treated with the CS adhesive and hydrogel (+CS) demonstrated an MRI signal and  $T_2$  signal change, whereas defects that were not treated with CS adhesive before hydrogel placement (-CS) were empty after 5 weeks ( $n = 3$ ). **b**, The CS-adhesive interface did not fracture when tensile and shear forces were applied. However, the hydrogel bulk failed when the adhesive was present (+CS). Without the CS adhesive (-CS), the hydrogel and cartilage separated easily at the interface. To determine the adhesive strength of the CS adhesive, highly crosslinked HEMA was bound to the cartilage surface and exposed to shear and tensile forces. The strength of the interface is presented in Table 1. **c-e**, Safranin-O staining of defects in the rabbit treated with CS adhesive and hydrogel (**c**), hydrogel alone (**d**) and no treatment (**e**) revealed enhanced proteoglycan deposition and tissue development when adhesive and hydrogel were present.

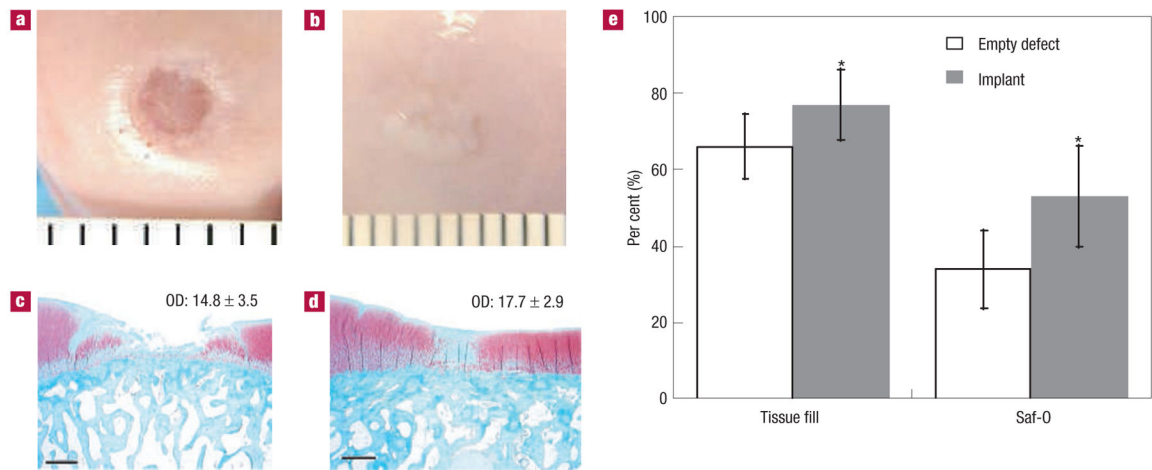


**Figure 5. CS adhesive and cartilage repair in a large-animal model.**

Two chondral defects (diameter 6mm) were created in the medial femoral condyle of goats. CS adhesive was placed in the defect after which the marrow was stimulated and the PEG hydrogel polymerized in the defect. **a,b**, Gross images of the empty control defects after 6 months showed minimal tissue fill (**a**) compared with defects treated with the gel and adhesive (**b**). **c,d**, Histological analysis confirmed that the gross pictures with the empty defect contained minimal tissue fill (**c**) compared with the treated defect (**d**). The majority of the tissue fill in the treated defects stained for Safranin-O, and the O'Driscoll (OD) score of the treated defects was greater than that of the controls (17.7 versus 14.8). The scale bars in **c,d** represent 1mm. **e**, Histomorphometric analysis quantified the area of tissue fill and positive Safranin-O staining and demonstrated statistically significant differences between the control and treated chondral defects ( $n = 6$  control defects,  $n = 12$  treated defects).



**Table 1**

Hydrogel–cartilage interface strength.

<b>Stress at interface failure</b>	<b>+CS primer</b>	<b>–CS primer</b>
Uniaxial tensile	45±2.0kPa	2.8kPa
Horizontal shear	46±1.7kPa	6.0kPa

*(n=5)*.

Author Manuscript

Author Manuscript

Author Manuscript

Author Manuscript